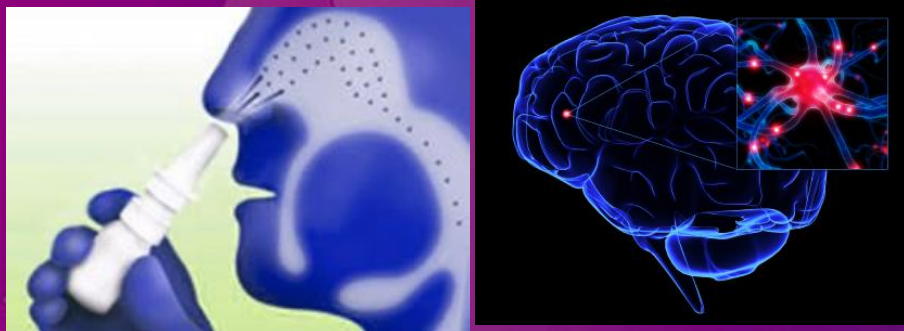




Nasal Route for CNS Drug Repurposing and Novel Delivery to the Brain

Prof. Joan Z. Zuo
School of Pharmacy, CUHK

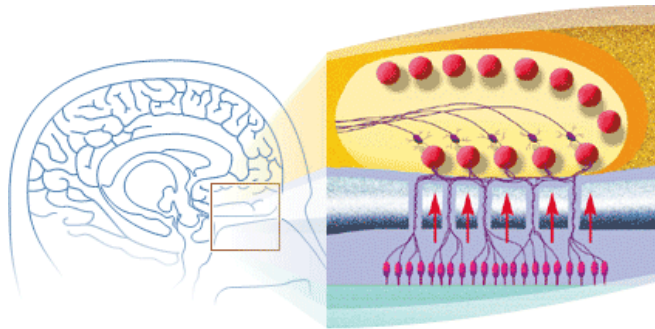
SOLVO Meet the Experts, Seoul, 2019



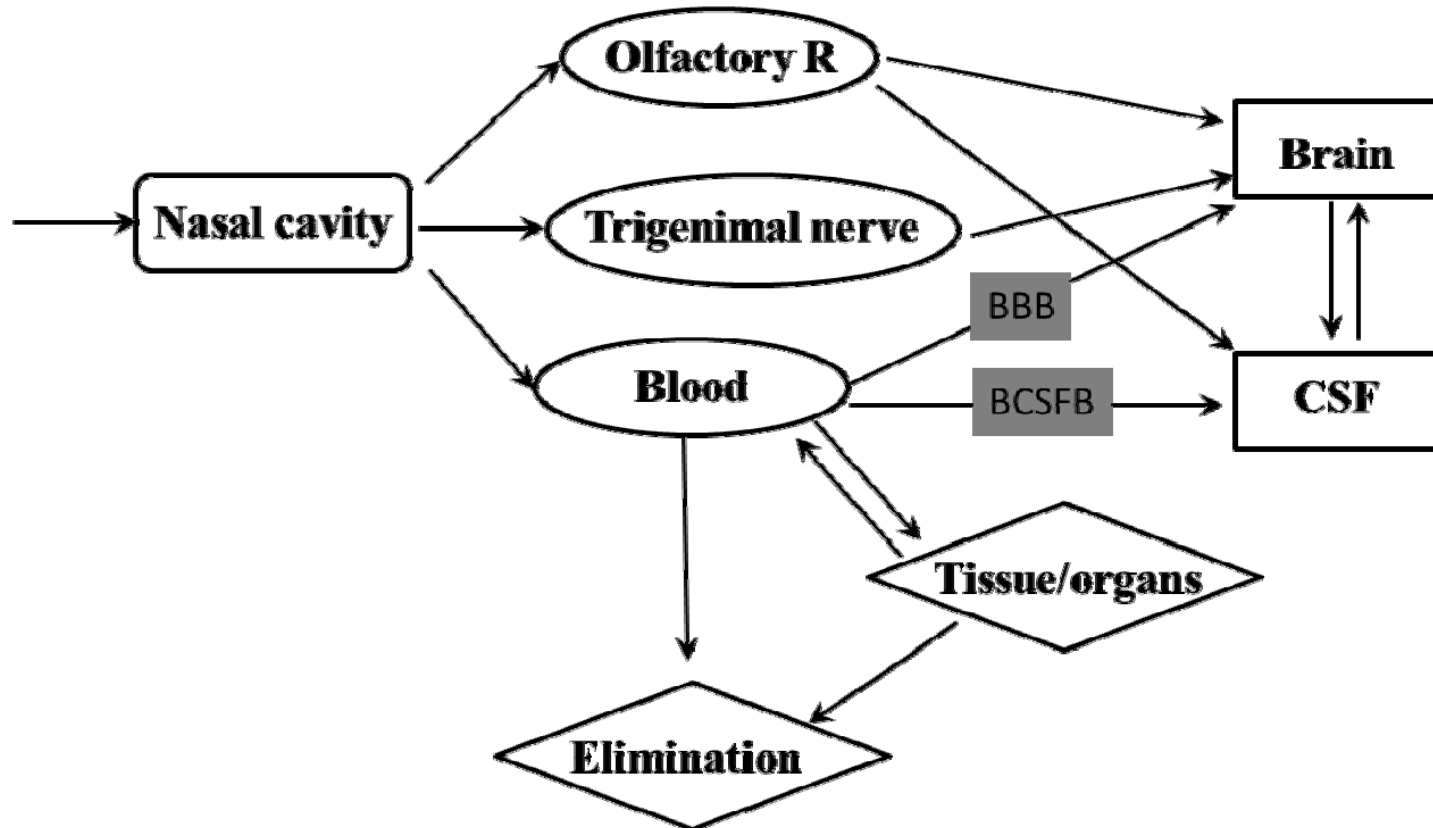
Nasal Delivery Advantages:

- Ability to **delivery** a wide range of therapeutics (small molecules and larger molecules such as peptides, proteins and nucleic acids)
- **Rapid** onset of action (critical to some disease states such as pain)
- **Avoidance of first-pass** hepatic metabolism
- Non-invasive compared to injection
- **Potential for direct delivery to the brain**





Direct-to-brain delivery of intranasal drugs may be facilitated by the incomplete blood-brain-barrier in the olfactory region.



BBB: blood-brain barrier; BCSFB: blood-cerebrospinal fluid barrier

What has been done for CNS targeting?

EXPERT OPINION

1. Introduction
2. Regioselectivity in metabolism
3. Toxicities of metabolites
4. Examples of toxic metabolites
5. *In silico* prediction of toxic metabolite formation
6. Strategies to modify metabolites formation
7. Expert opinion

Pharm Res (2010) 27:1208–1223
DOI 10.1007/s1095-010-0127-5

COMMENTARY

Intranasal Delivery—Modification of Drug Metabolism and Brain Disposition

Yin Cheong Wong • Zhong Zuo

Review

Regioselective biotransformation of CNS drugs and its clinical impact on adverse drug reactions

Yin Cheong Wong, Shuai Qian & Zhong Zuo

[†]The Chinese University of Hong Kong, School of Pharmacy, Hong Kong SAR

Introduction: Adverse drug reactions (ADRs) cause failure in drug development with many drugs. Contribution of the metabolites to ADRs may be more significant than we might have expected.

Areas covered: This review focuses on the importance of regioselectivity in biotransformation and the ADRs of CNS drugs. “Regioselectivity” is defined as a preferential metabolic reaction at one (or more) site(s) of CNS drugs and ADRs.

EXPERT OPINION

1. Introduction
2. Brain barriers of CNS peptide delivery
3. Brain uptake and

Review

Improved brain uptake of peptide-based CNS drugs via alternative routes of administrations of its nanocarrier delivery systems: a promising strategy for CNS targeting delivery of peptides

Shuai Qian, Qianwen Wang & Zhong Zuo[†]

[†]The Chinese University of Hong Kong, School of Pharmacy, Faculty of Medicine, Shatin, N.T., SAR, Hong Kong

Introduction: Recently, developing peptide-based drugs to treat CNS diseases has gained increasing attention in both academics and pharmaceutical industry. However, targeting delivery of peptides to brain is one of the most challenging problems faced in the treatment of CNS diseases.

CNS drugs (small molecules)

- Phase I and Phase II metabolisms not only detoxify the xenobiotics but might also contribute to the ADRs by generating toxic metabolites which have been observed in many CNS drugs.
- Regioselectivity in biotransformation deserves more attention since selective formation or elimination of the toxic metabolites would play an important role in intensifying or mitigating the ADRs.
- Structural modifications of drug candidates and **alternative routes of drug delivery** are **effective approaches** to modify metabolite formation.



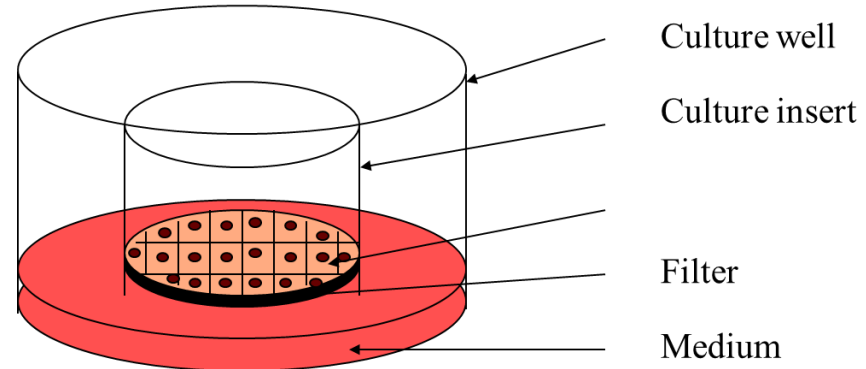
Protein drugs

- Poor penetration across the blood brain barrier (BBB) is the major limitation of peptides as therapeutic agents for the treatment of CNS diseases.
- **Alternative routes of administrations especially intranasal delivery** of peptides demonstrated its unique advantage to deliver peptide based CNS drugs into brain leading to improvement in both their pharmacokinetics and pharmacodynamics.
- Taking advantages of both **nanocarriers** and **intranasal route** of administration have demonstrated significant improvement in brain uptake of peptide than any other traditional approaches for CNS targeting delivery of peptides.

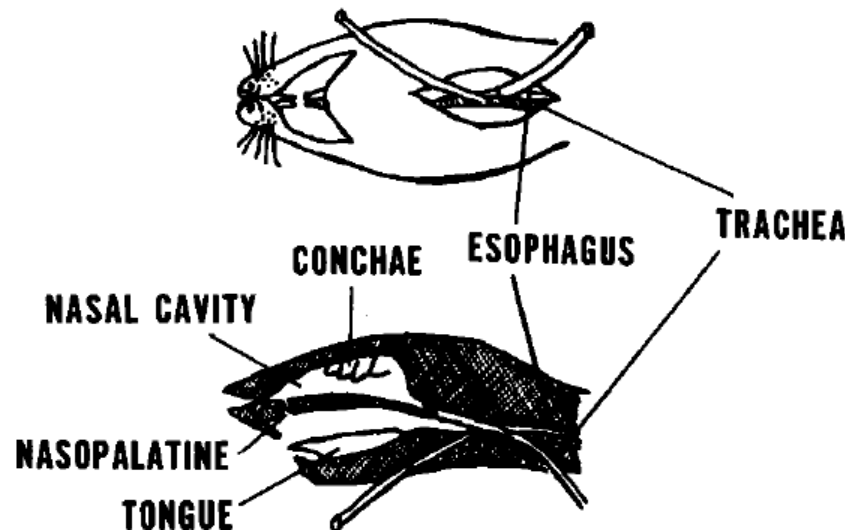


Commonly used study models for intranasal delivery

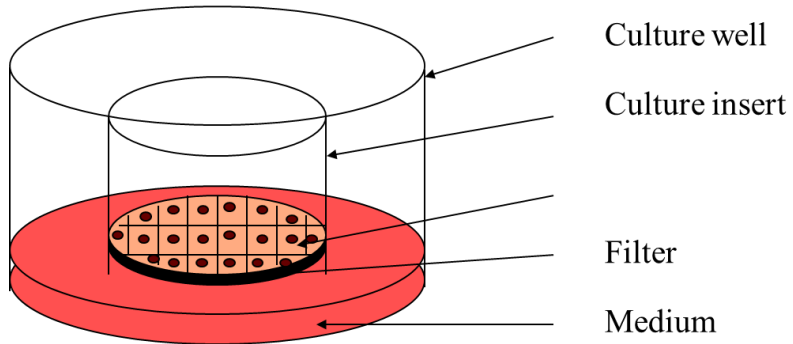
- In-vitro cell model
- In-situ animal model
- In-vivo animal model



Rat Model



In vitro cell line models



International Journal of Pharmaceutics 420 (2011) 43–50



Contents lists available at ScienceDirect

International Journal of Pharmaceutics

Journal homepage: www.elsevier.com/locate/ijpharm

An approach for rapid development of nasal delivery of analgesics—Identification of relevant features, *in vitro* screening and *in vivo* verification

Shu Wang^a, Moses S.S. Chow^b, Zhong Zuo^{a,*}

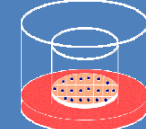
^aSchool of Pharmacy, Faculty of Medicine, The Chinese University of Hong Kong, Shatin, New Territories, Hong Kong Special Administrative Region

^bCenter for Advancement of Drug Research and Evaluation, College of Pharmacy, Western University of Health Sciences, Pomona, CA, USA

Selection of analgesics for nasal delivery :

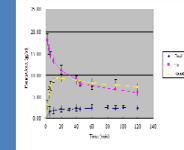
- physicochemical properties;
- clinical usage

Screening of candidates using validated Calu-3 cell model



The most potent candidate for *in vivo* verification:

- i.v. administrations ;
- oral administrations;
- nasal administrations;



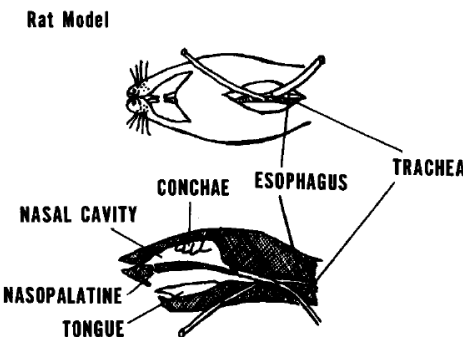
Choose Appropriate Rat Model

Pharm Res
DOI 10.1007/s11095-014-1312-8

RESEARCH PAPER

Pharmacokinetic Comparison Between the Long-Term Anesthetized, Short-Term Anesthetized and Conscious Rat Models in Nasal Drug Delivery

Yin Cheong Wong • Shuai Qian • Zhong Zuo



VS





香港中文大學
The Chinese University of Hong Kong



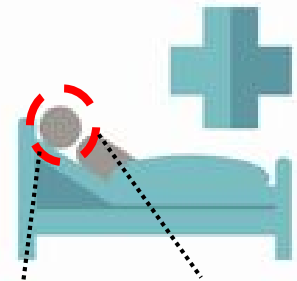
香港中文大學醫學院
Faculty of Medicine
The Chinese University of Hong Kong



CASE STUDIES

Intranasal Delivery Targeting Polyglutamine Diseases

Background-PolyQ diseases



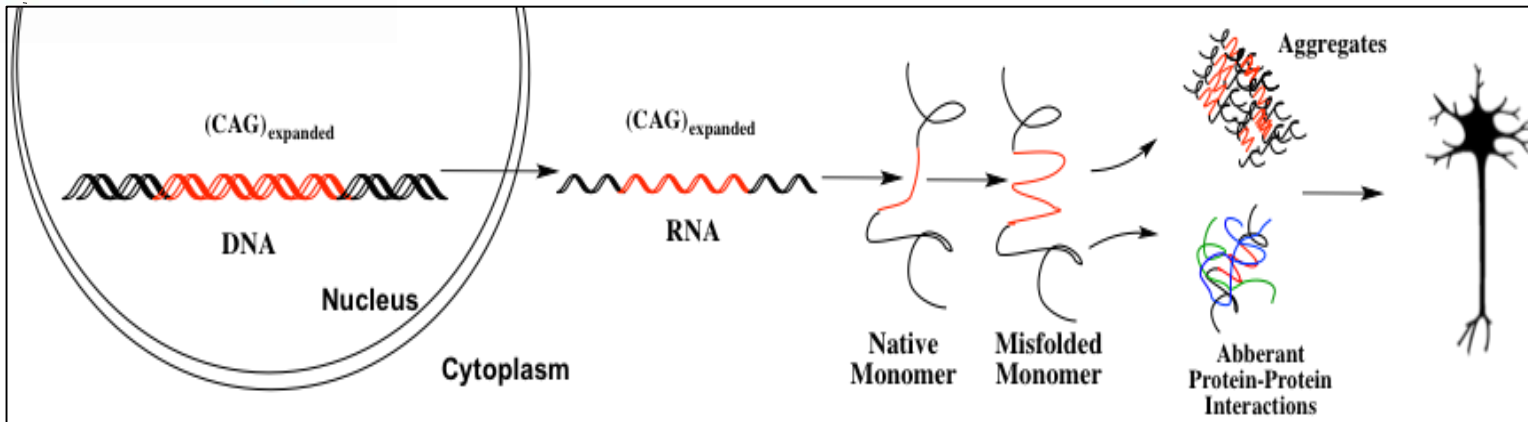
Huntington's

Spinocerebellar ataxia
(SCA) type 1, 2, 3, 6, 7,

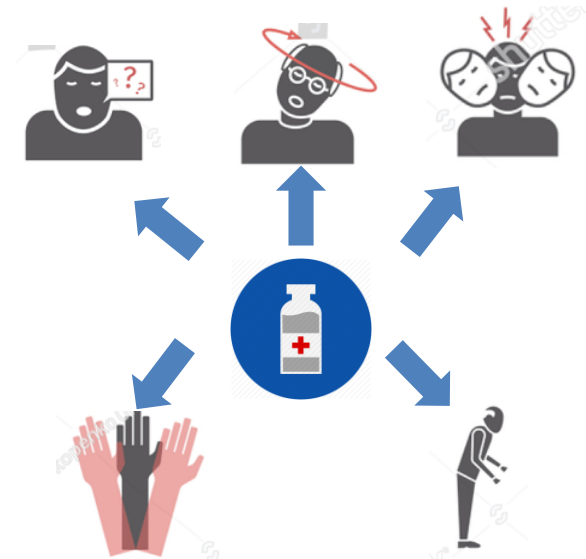
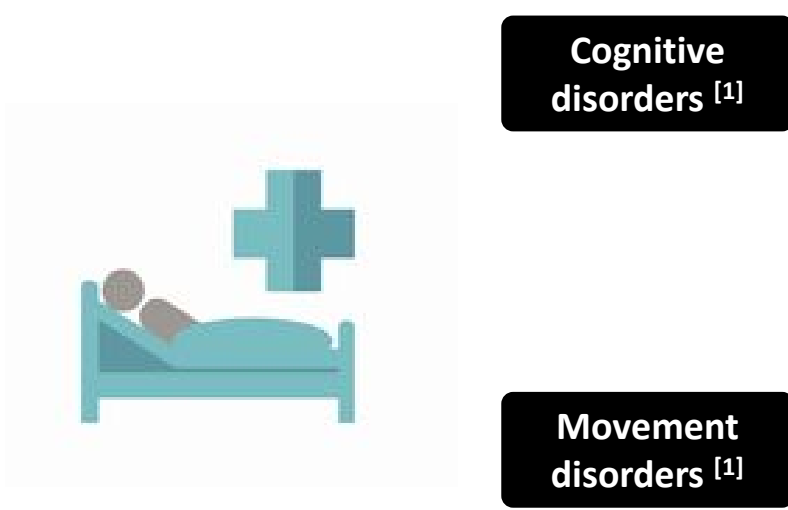
(SBMA)

(DRPLA)

PolyQ diseases are a group of neurodegenerative disorders caused by expanded CAG RNA encoding a long polyQ tract in brain cells.



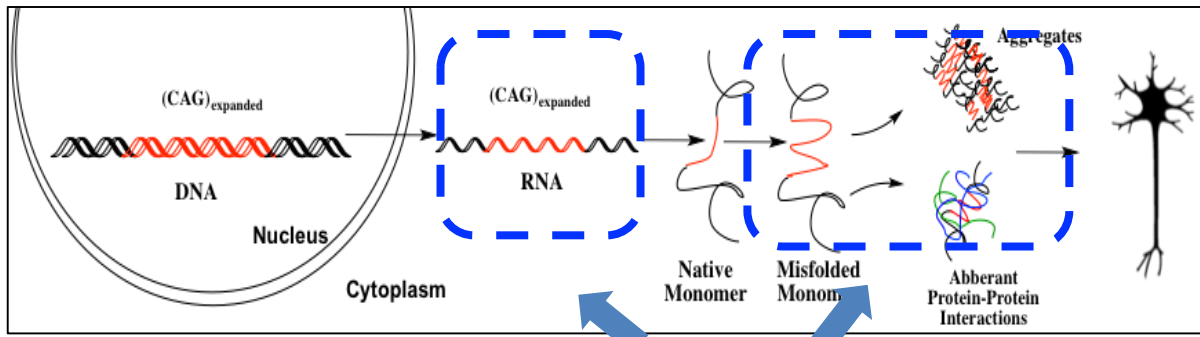
Background: PolyQ diseases



No effective clinical treatment based on the pathogenesis of polyQ diseases

[1] Guo F, Liu X, Cai H, et al. Brain Pathology, 2018, 28(1): 3-13.

Background: PolyQ diseases



Human neuronal cell line [2]



Drosophila disease model [2]

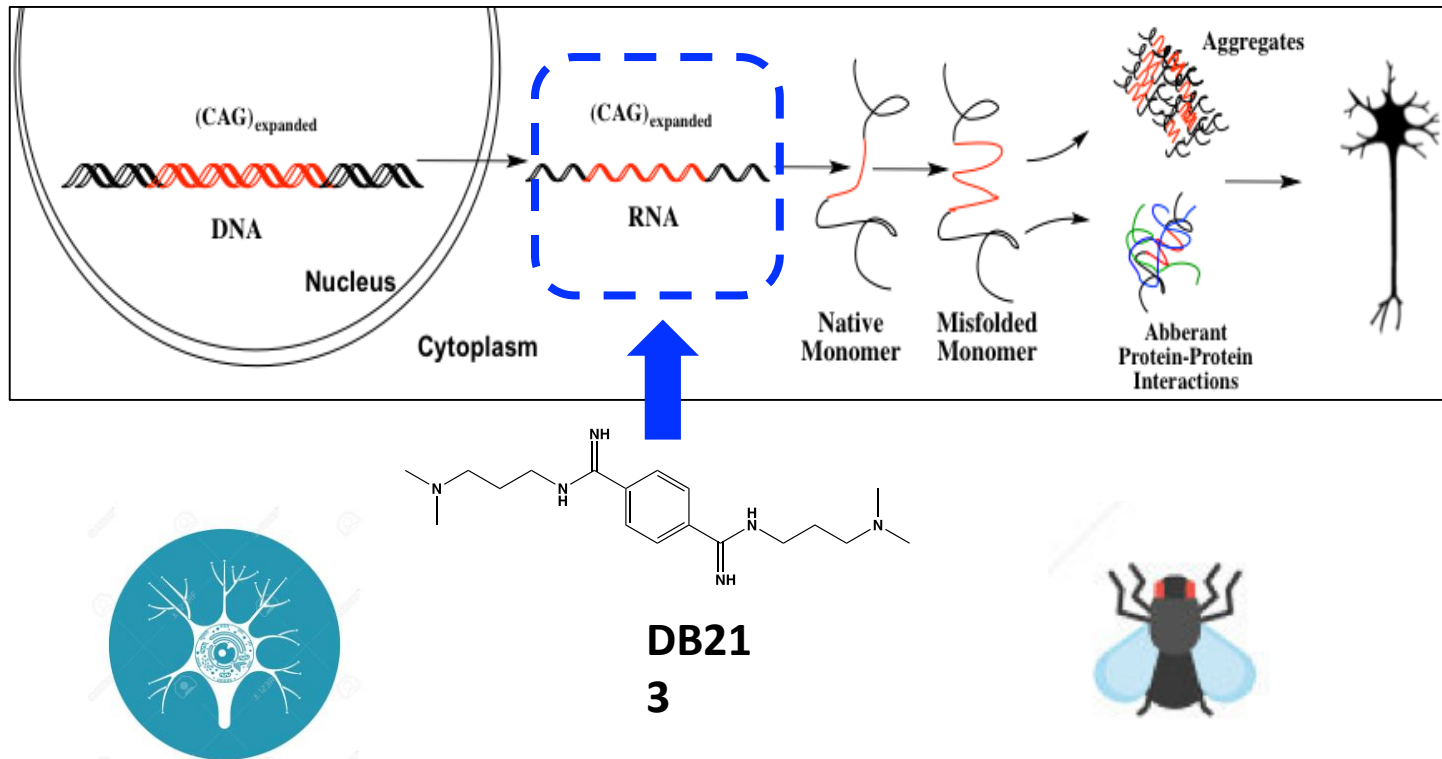


R6/2 Huntington's disease mice model [3]

[2] Jackson G R, Salecker I, Dong X, et al. Neuron, 1998, 21(3): 633-642. [3] Luthi-Carter R, Hanson S A, Strand A D, et al. Human molecular genetics, 2002, 11(17): 1911-1926.

HOW TO DELIVER SMALL MOLECULE DRUG CANDIDATE?

Background: DB213

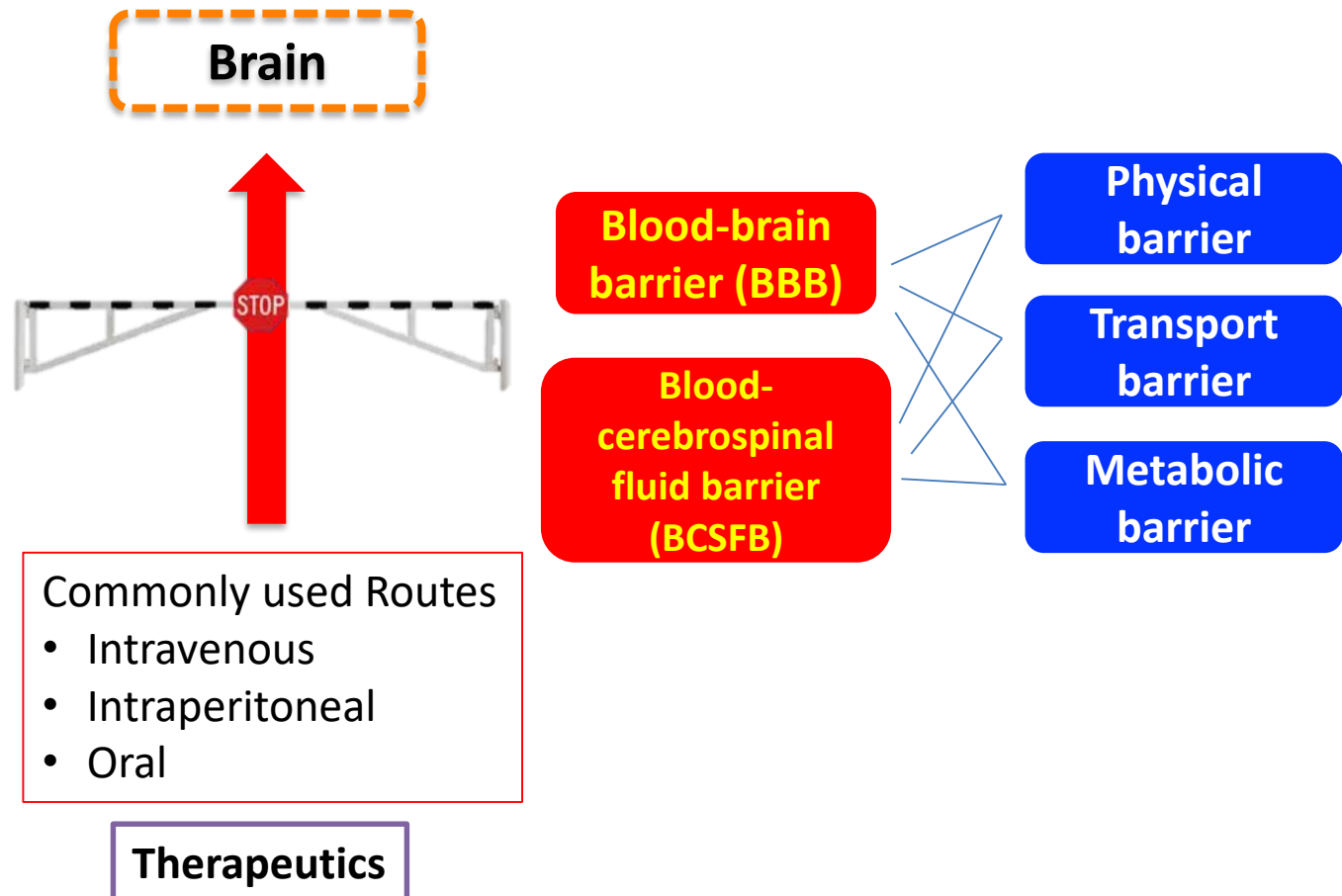


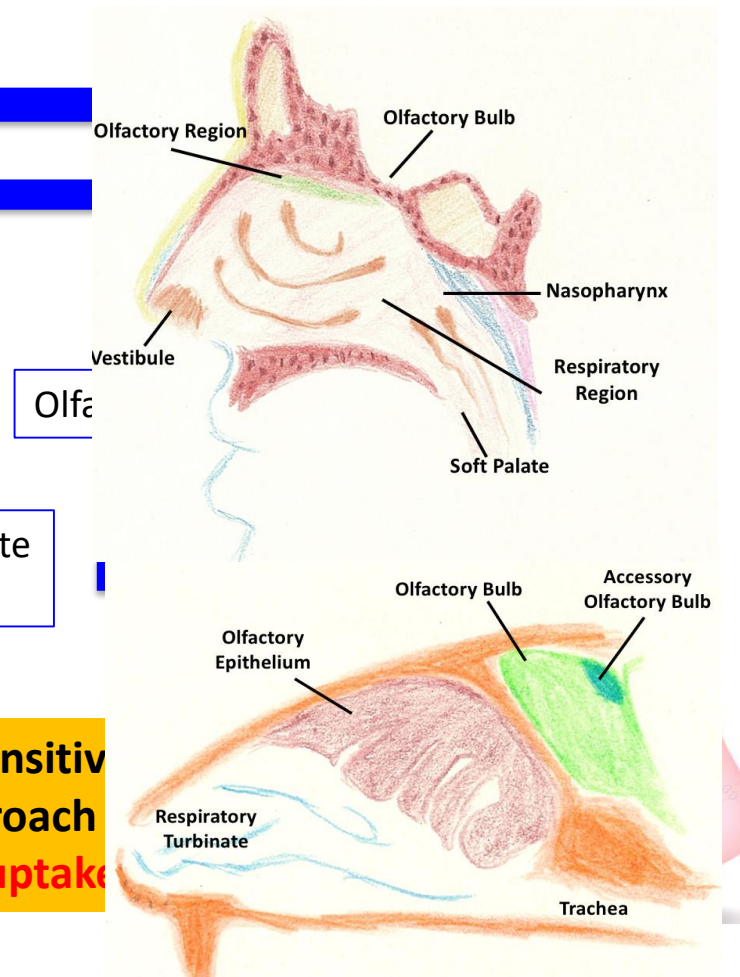
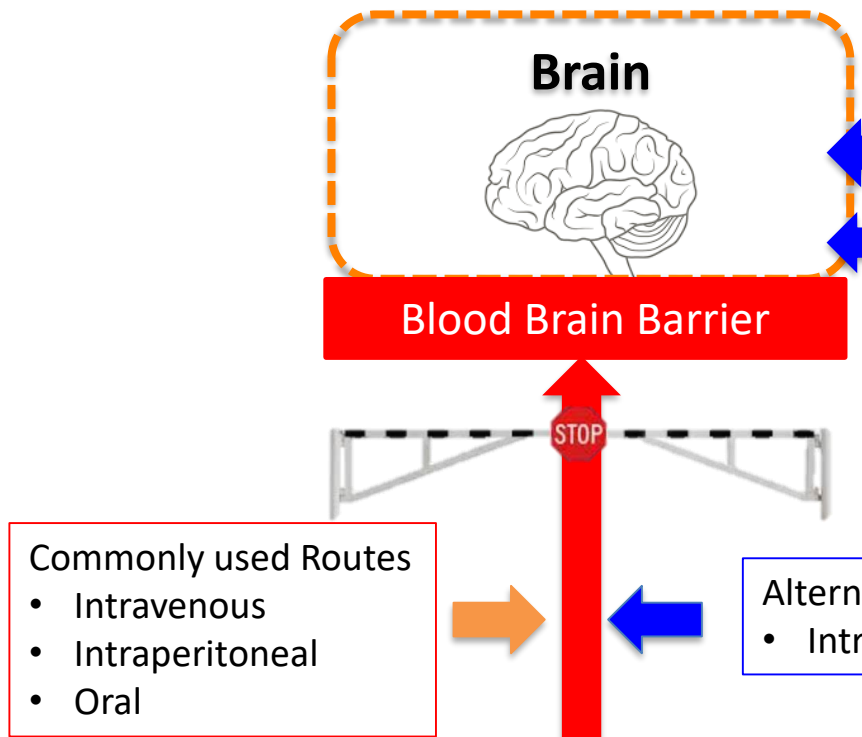
Human neuronal cell line [4]

Drosophila disease model [4]

DB213 is a **promising** CAG-repeated RNA inhibitor targeting polyQ diseases on its **pathogenesis bases** [4].

Background: Barriers for drug delivery in the brain





Intranasally administered in-situ thermosensitive
alternative and noninvasive drug delivery approach
enhance drug brain uptake



Marvin
ACD/Labs



In-silico prediction

Compound	BBB permeability predictions										
	LogP ^a	pKa ^b	1 ^c	2 ^d	3 ^d	4 ^d	5 ^d	6 ^d	7 ^d	8 ^d	9 ^d
DB213	1.57	9.80	BBB-	-0.94 (BBB-)	14.91 (BBB+)	6.21 (BBB+)	5.17 (BBB+)	-0.005 (BBB-)	0.28 (BBB+)	0.83 (BBB+)	0.11 (BBB+)
Diazepam	2.82	3.41	BBB+	7.82 (BBB+)	23.18 (BBB+)	10.85 (BBB+)	14.39 (BBB+)	0.13 (BBB+)	0.22 (BBB+)	0.56 (BBB+)	0.26 (BBB+)
Doxorubicin	1.27	8.46	BBB-	-5.30 (BBB-)	-16.03 (BBB-)	-11.89 (BBB-)	-14.83 (BBB-)	-0.29 (BBB-)	-1.21 (BBB-)	-0.35 (BBB-)	-1.11 (BBB-)

^a: value predicted by ChemBioDraw

^b: value predicted by MarvinSketch

^c: value predicted by ACD/Labs

^d: value predicted by online BBB predictor using different algorithms (AdaBoost and SVM) and fingerprint databases (MACCS, Openbabel, Molprint2D and PubChem): 2 (AdaBoost and MACCS), 3(AdaBoost and Openable), 4(AbaBoost and Molprint2D), 5(AdaBoost and PubChem), 6(SVMand MACCS), 7(SVM and Openable), 8(SVM and Molprint2D), and 9 (SVM and PubChem).

***In silico* prediction showed DB213 has limited BBB permeability**

Nasal epithelium permeability

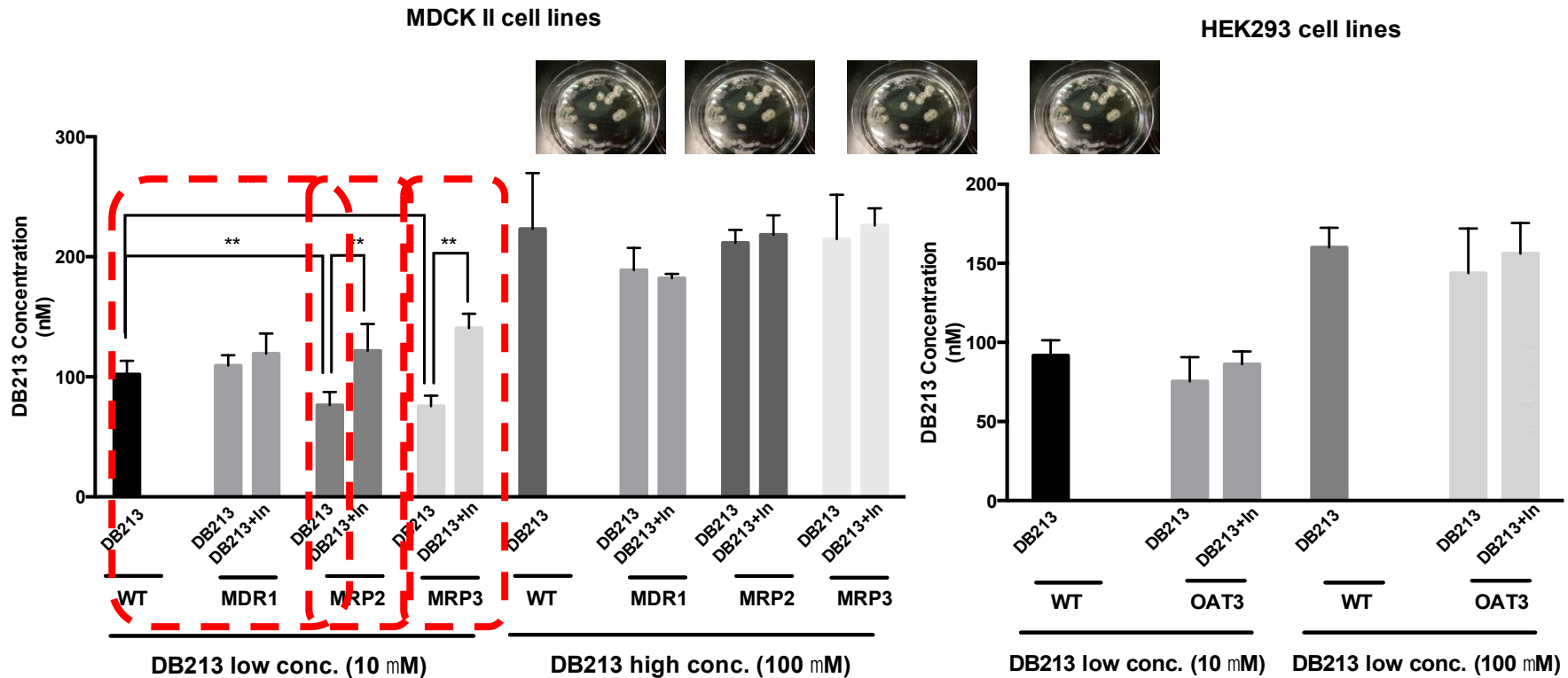
Compound	Loading concentration (μM)	Calu-3 $P_{\text{app}(a \rightarrow b)}$ ($\times 10^{-6} \text{ cm/s}$)		Cell uptake (%) (n=3)
		Experimental value (n=3)	Reference value ^[8]	
Propranolol	100	15.76 ± 1.95	22.70 ± 5.50	0.92
Atenolol	200	0.13 ± 0.02	0.1 ± 0.01	1.98
DB213	10	1.40 ± 0.21	N.A.	3.55 ± 1.14
	100	1.87 ± 0.29	N.A.	3.10 ± 1.43
	300	1.98 ± 0.48	N.A.	4.35 ± 1.74

DB213

Calu-3 monolayer cell model

DB213 has limited nasal epithelium permeability

Potential transporters



DB213 is identified as substrate of MRP2 and MRP3 efflux transporters

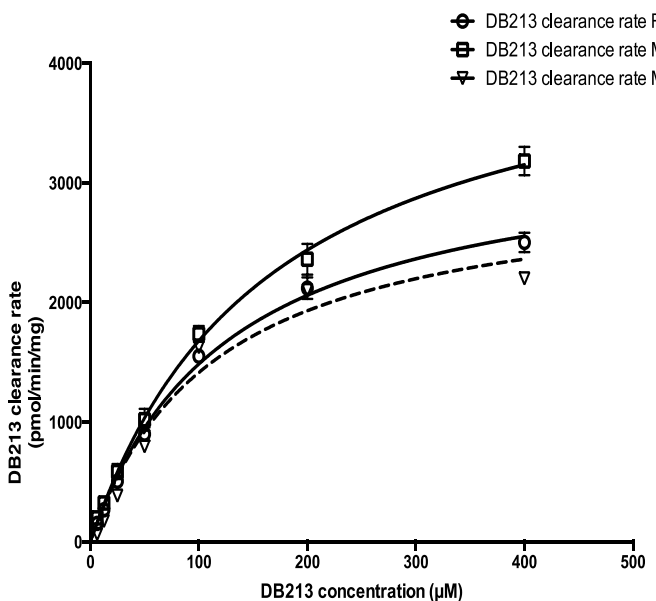
Plasma and tissue binding

Binding (%)	DB213 Spiked Conc.	SD rat			C57 mice	R6/2 mice
Plasma (n=3)	Incubation Time	2 h	4 h	17 h	2 h	2 h
	0.3 ($\mu\text{g/mL}$)	3 \pm 3	1 \pm 4	1 \pm 4	26 \pm 10	30 \pm 5
	3 ($\mu\text{g/mL}$)	2 \pm 3	1 \pm 5	0 \pm 3	21 \pm 5	28 \pm 11
	30 ($\mu\text{g/mL}$)	0 \pm 5	2 \pm 5	2 \pm 4	19 \pm 5	17 \pm 8
	300 ($\mu\text{g/mL}$)	3 \pm 7	2 \pm 3	1 \pm 2	17 \pm 9	12 \pm 5
Brain tissue (n=3)	2 h	4 h	17 h	4 h	4 h	
	50 (ng/g)	90 \pm 0.5	96 \pm 0.3	96 \pm 0.6	89 \pm 1	89 \pm 1
	500 (ng/g)	92 \pm 0.3	96 \pm 0.3	95 \pm 0.2	87 \pm 5	90 \pm 1
	5000 (ng/g)	93 \pm 0.6	95 \pm 0.4	95 \pm 0.2	87 \pm 1	90 \pm 1

DB213 demonstrated **low** protein binding (less than 30%) **in plasma** and rather **high** protein (greater than 85%) **in brain homogenate**



Phase I metabolism



Type of microsomes	V_{\max} (nmol/min/mg)	K_m (mM)	CL_{in} ($\mu\text{L}/\text{min}/\text{mg}$)
RLM	3357 ± 130	126 ± 14	26.64
MLM (C57)	4451 ± 136	165 ± 11	26.98
MLM (R6/2)	4410 ± 104	206 ± 77	21.41

DB213

CL_{in} of other drugs ($\mu\text{L}/\text{min}/\text{mg}$)

- felodipine: 500
- propranolol: 3120
- imipramine 4500^[9]

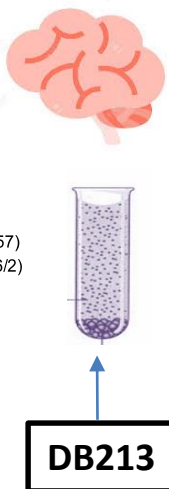
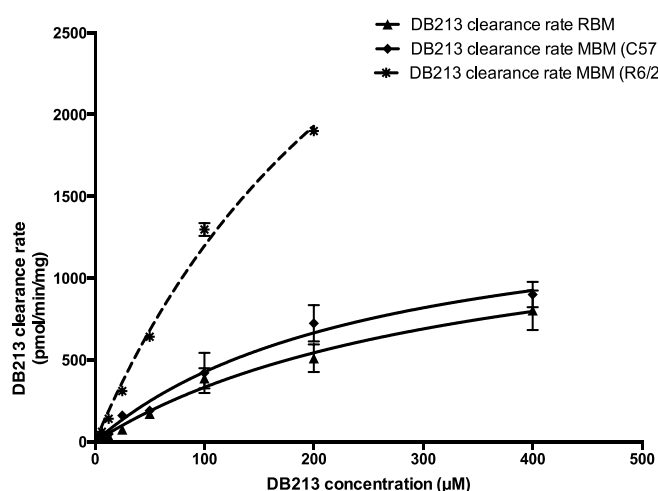
Phase II metabolism

- <5% DB213 was metabolized by Phase II glucuronidation
- <15% DB213 was metabolized by Phase II sulfation

DB213 demonstrated limited liver metabolism in rats and mice

^[9] Wager T T, Hou X, Verhoest P R, et al. ACS chemical neuroscience, 2010, 1(6): 435-449.

Phase I metabolism



Type of microsome	V_{max} (nmol/min/mg)	K_m (mM)	CL_{in} (mL/min/mg)
RBM	1490 ± 116	348 ± 57	4.28
MBM (C57)	1517 ± 89	256 ± 61	5.92
MBM (R6/2)	4968 ± 102	314 ± 94	15.82

- imipramine: 3000 μL/min/mg [9]

Phase II metabolism

- <1% DB213 was metabolized by Phase II glucuronidation

DB213 demonstrated limited brain metabolism in rats and mice

DB213 NEEDS SERIOUS HELP !!!!

The AAPS Journal (2018) 20: 23
DOI: 10.1208/s12248-017-0179-0



Research Article

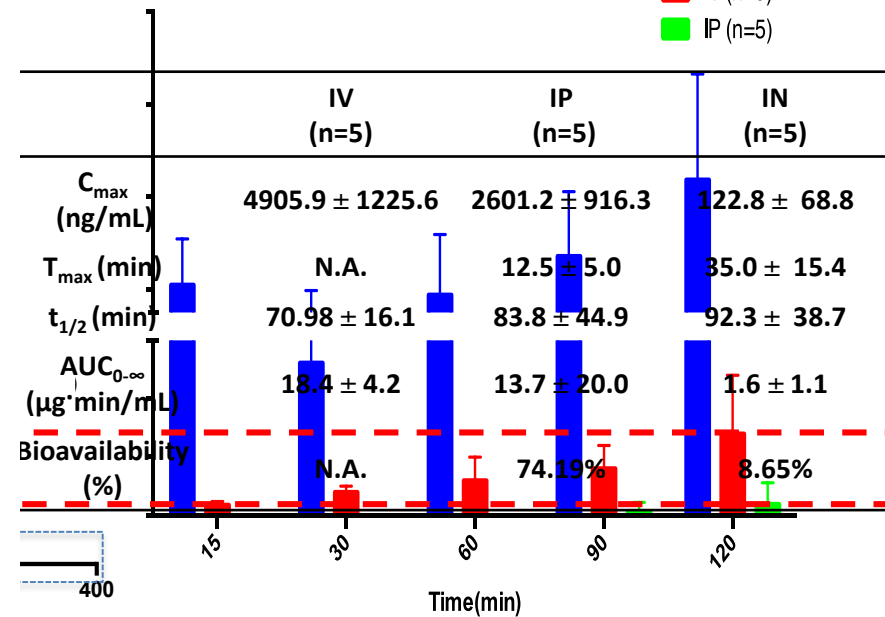
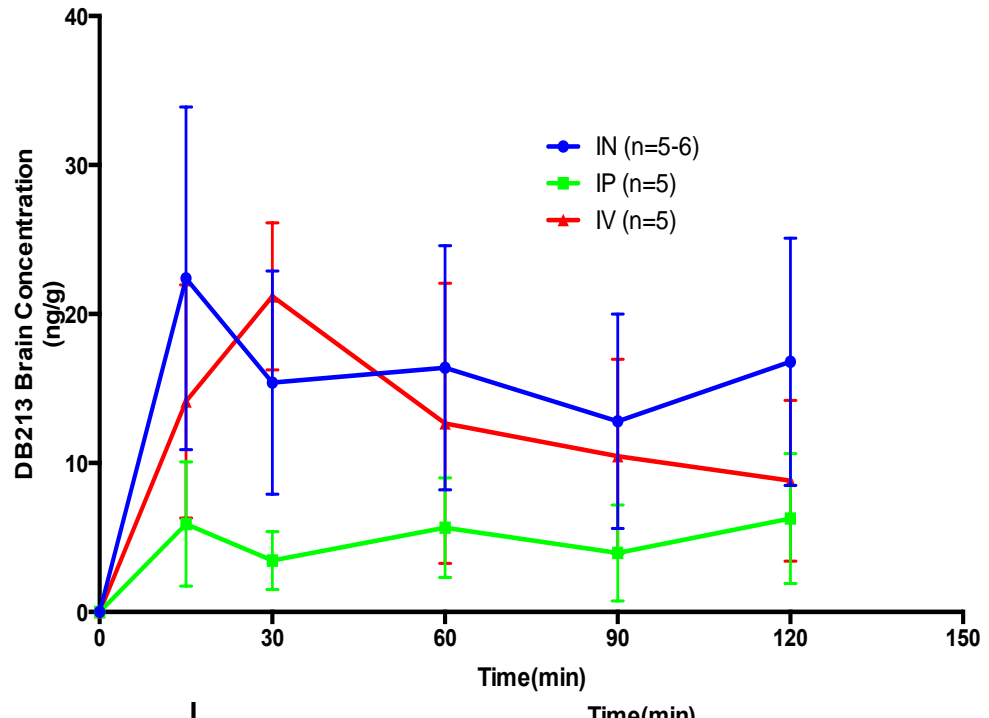
Demonstration of Direct Nose-to-Brain Transport of Unbound HIV-1 Replication Inhibitor DB213 Via Intranasal Administration by Pharmacokinetic Modeling

Qianwen Wang,¹ Yufeng Zhang,¹ Chun-Ho Wong,² H.Y. Edwin Chan,^{2,3} and Zhong Zuo^{1,4}

Which route of administration?

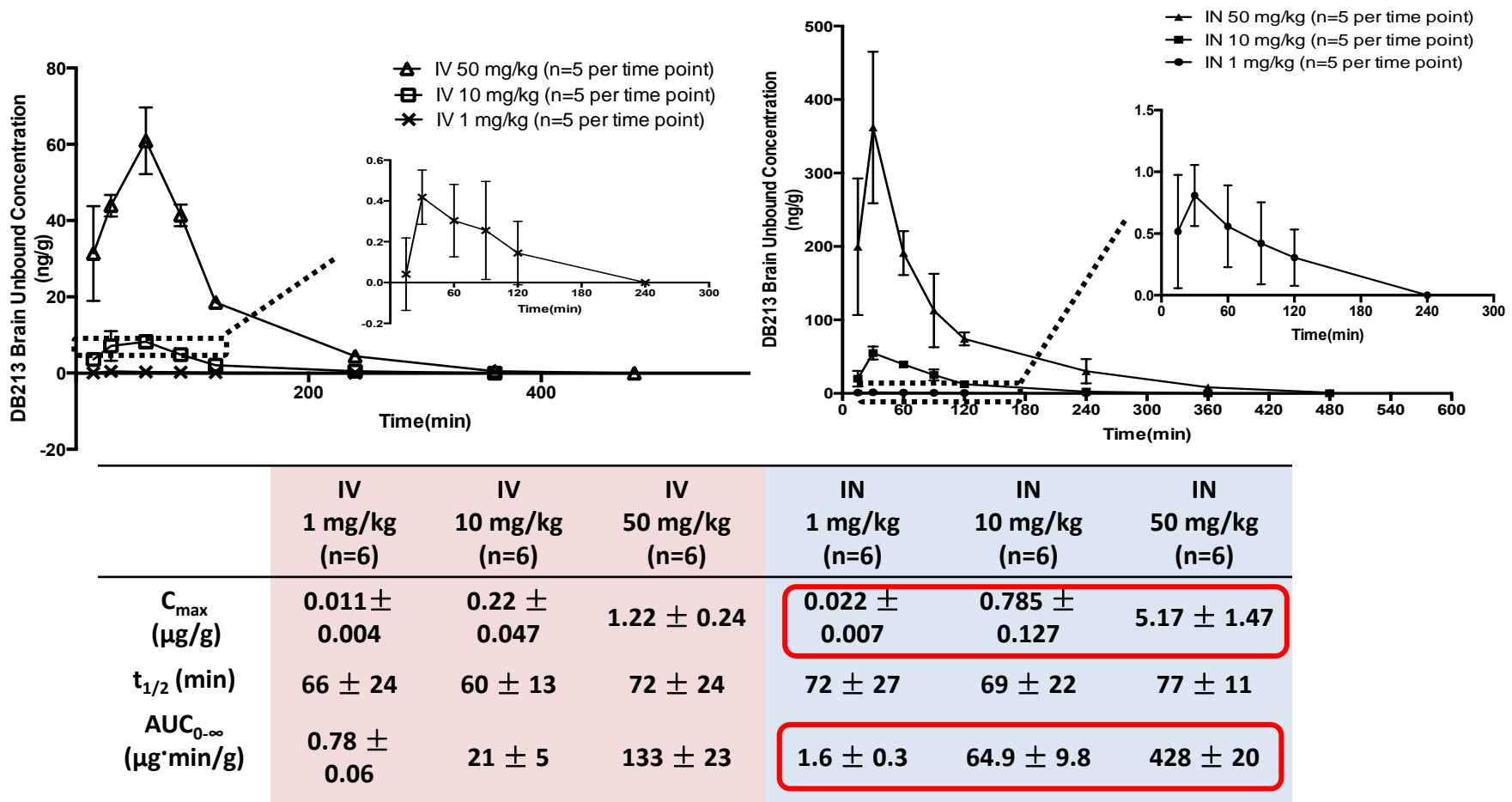
IN VIVO EVALUATION IN SD RATS

Intranasal as best route for CNS delivery of DB213

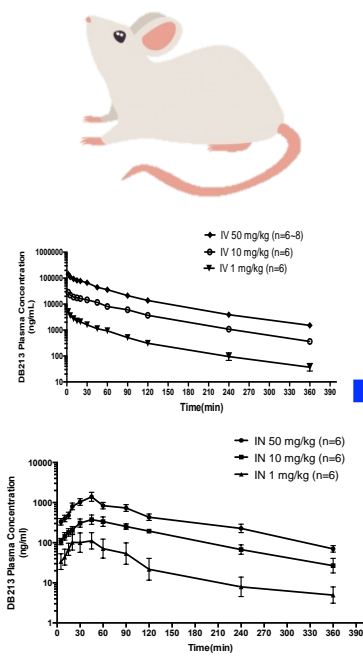


Intranasal administration has a potential to enhance brain uptake of DB213

Dose dependency of DB213: Brain



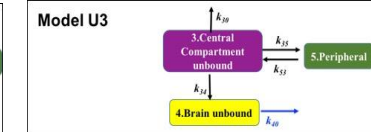
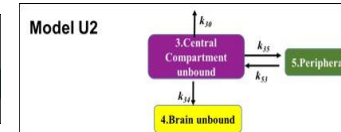
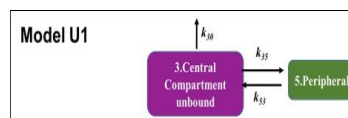
Demonstration of direct nose-to-brain transport by PK modeling



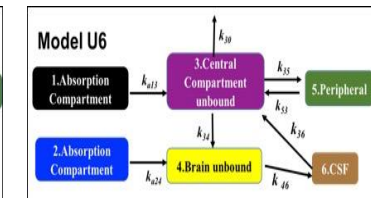
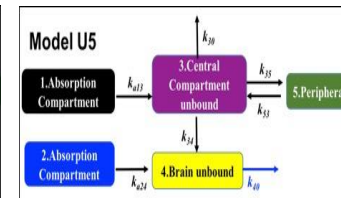
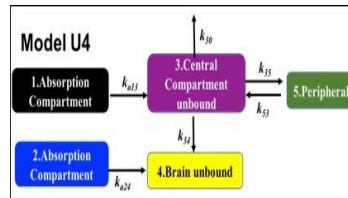
NONMEM™

The program for Nonlinear Mixed Effects Modeling

Pharmacokinetics (PK) model of DB213 via **intravenous** route

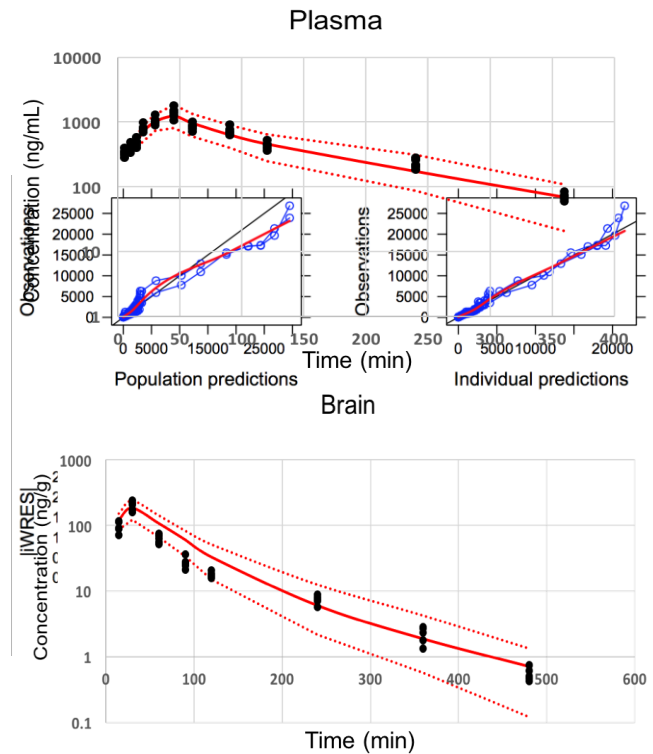
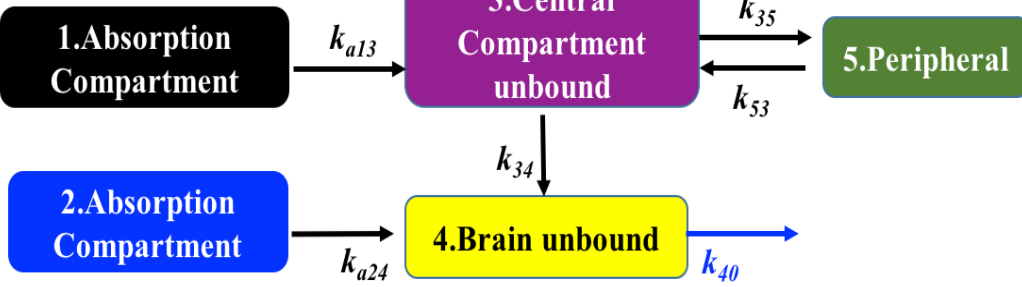


Pharmacokinetics (PK) model of DB213 via **intravenous** and **intranasal** route



Demonstration of direct nose-to-brain transport of DB213

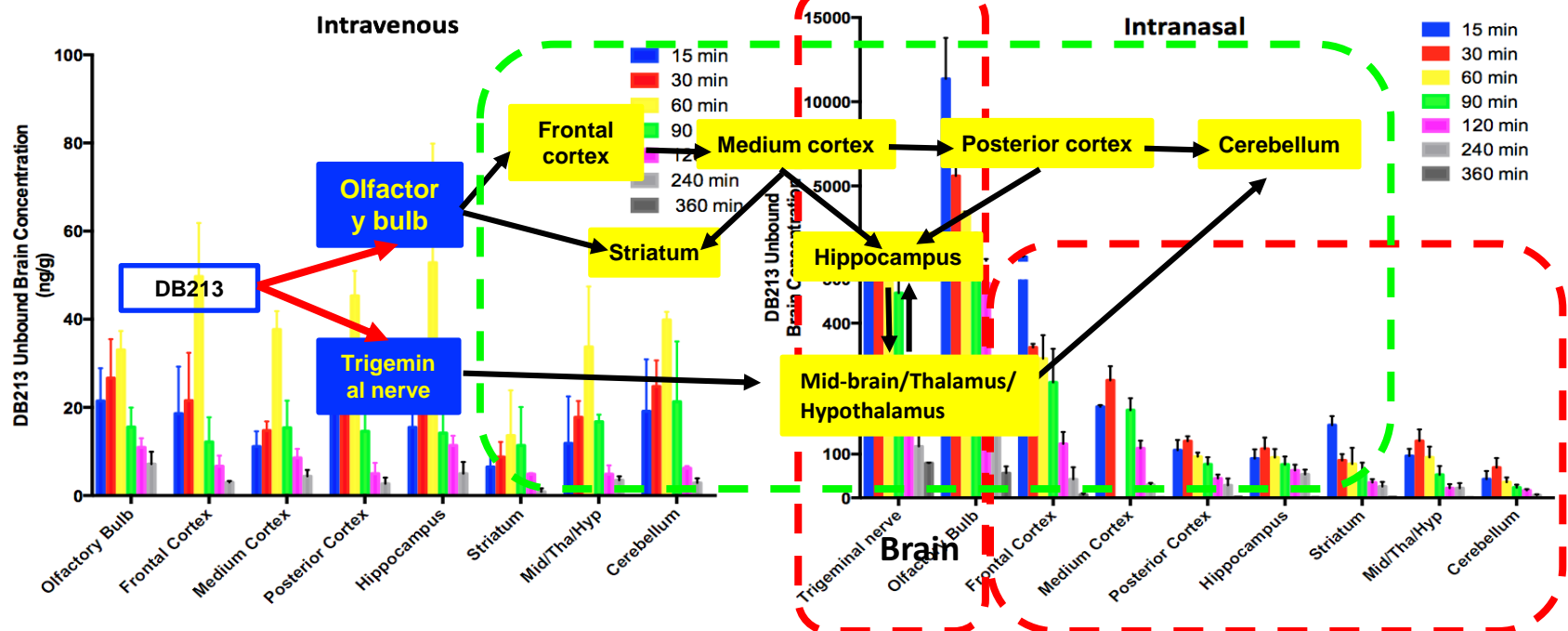
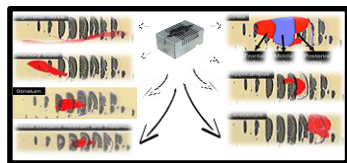
Model U5



PK modeling suggested that **direct nose-to-brain pathway** is responsible for delivering **70.7%** of the absorbed DB213 to the brain^[10].

^[10] Wang Q, Zhang Y, Wong C H, et al. The AAPS journal, 2018, 20(1): 23.

Brain regional distribution of DB213



Both **olfactory bulb** and **trigeminal nerve** could serve as entry point of nose-to-brain delivery of DB213 followed by its diffusion into other brain regions.

European Journal of Pharmaceutical Sciences 127 (2019) 240–251

Contents lists available at ScienceDirect

European Journal of Pharmaceutical Sciences

journal homepage: www.elsevier.com/locate/ejps

 ELSEVIER



Efficient brain uptake and distribution of an expanded CAG RNA inhibitor DB213 via intranasal administration

Qianwen Wang^a, Shaohong Peng^b, Yue Hu^b, Chun-Ho Wong^b, Kin Ming Kwan^b, H.Y. Edwin Chan^{b,c}, Zhong Zuo^{b,*}

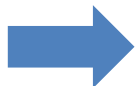
^a School of Pharmacy, The Chinese University of Hong Kong, Shatin, N.T., Hong Kong

^b School of Life Sciences, The Chinese University of Hong Kong, Shatin, N.T., Hong Kong

^c Gerald Choa Neuroscience Centre, The Chinese University of Hong Kong, Shatin, N.T., Hong Kong



FORMULATION DEVELOPMENT



Design Phase

Exp No	Exp Name	Run Order	water (w/w)	DB213 (w/w)	Chitosan (w/w)	PF-68 (w/w)	PF-127 (w/w)
1	N1	24	0.78	0.01	0	0.01	0.2
2	N2	5	0.655	0.05	0.00499999	0.01	0.28
3	N3	1	0.655	0.01	0.005	0.03	0.3
4	N4	21	0.775	0.01	0.00499999	0.01	0.2
5	N5	8	0.76	0.01	0	0.03	0.2
6	N6	16	0.755	0.01	0.00499999	0.03	0.2
7	N7	14	0.715	0.05	0.00499999	0.03	0.2
8	N8	15	0.675	0.01	0.005	0.01	0.3
9	N9	3	0.66	0.01	0	0.03	0.3
10	N10	9	0.655	0.05	0	0.0166667	0.278333
11	N11	10	0.655	0.0216667	0	0.0233333	0.3
12	N12	20	0.713333	0.01	0	0.01	0.266667
13	N13	19	0.711667	0.05	0	0.01	0.228333
14	N14	25	0.726667	0.05	0	0.0233333	0.2
15	N15	4	0.733333	0.0366667	0	0.03	0.2
16	N16	23	0.655	0.05	0.00166666	0.03	0.263333
17	N17	12	0.655	0.05	0.00333333	0.03	0.261667
18	N18	7	0.655	0.0233333	0.00499999	0.03	0.286667
19	N19	11	0.655	0.0333334	0.00166666	0.01	0.3
20	N20	17	0.736667	0.05	0.00333333	0.01	0.2
21	N21	18	0.7175	0.01	0.0025	0.02	0.25
22	N22	13	0.697222	0.03	0.00499999	0.0188889	0.248889
23	N23	6	0.696579	0.0294737	0.00236842	0.0194737	0.252105
24	N24	2	0.696579	0.0294737	0.00236842	0.0194737	0.252105
25	N25	22	0.696579	0.0294737	0.00236842	0.0194737	0.252105



Analysis phase

Factors
A: PF-127
B: PF-68
C: Chitosan
D: DB213

- $T_{\text{sol-gel}}$
 - Best fit with MLR model
 - $T_{\text{sol-gel}} = 36.59 + 0.22A^2 + 1.12A - 2.25B^2 - 1.31D$
- ***In vitro* release at 1 h**
 - Best fit with PLS model
 - ***In vitro* release at 1 h=**
 $37.42 - 0.62A + 9.56B - 1.52AB + 6.9B^2 + 6.14C^2$
- **Mucoclearnace time**
 - Best fit with MLR model
 - **Mucoclearnace time=**
 $21.30 + 11.3C + 5.68BC + 1.23AC$

DOE for in-situ gel development



Prediction phase for SD rat

Formulation predictions:

- PF-127: 27.99%
- PF-68: 2.87%
- Chitosan: 0.5%
- DB213: 1%

Target

- $T_{sol-gel}$: 31°C
- *In vitro* release at 1 h: >60%
- Mucoclearance time (MCT): >30 min
- DB213 amount at 1%



Performance predictions

- $T_{sol-gel}$: 31°C
- *In vitro* release at 1 h: 75%
- MCT: 54 min

Performance Observations

- $T_{sol-gel}$: $32.2 \pm 0.3^\circ\text{C}$
- *In vitro* release at 1 h: $71 \pm 4.3\%$
- MCT: 50 ± 5 min

Results: DOE for in-situ gel development



Prediction phase for C57 and R6/2 mice

Formulation predictions:

- PF-127: 24.99%
- PF-68: 2.07%
- Chitosan: 0.5%
- DB213: 5%

Target

- $T_{sol-gel}$: 31°C
- *In vitro* release at 1 h: >60%
- Mucoclearance time (MCT): >30 min
- DB213 amount at 5%



Performance predictions

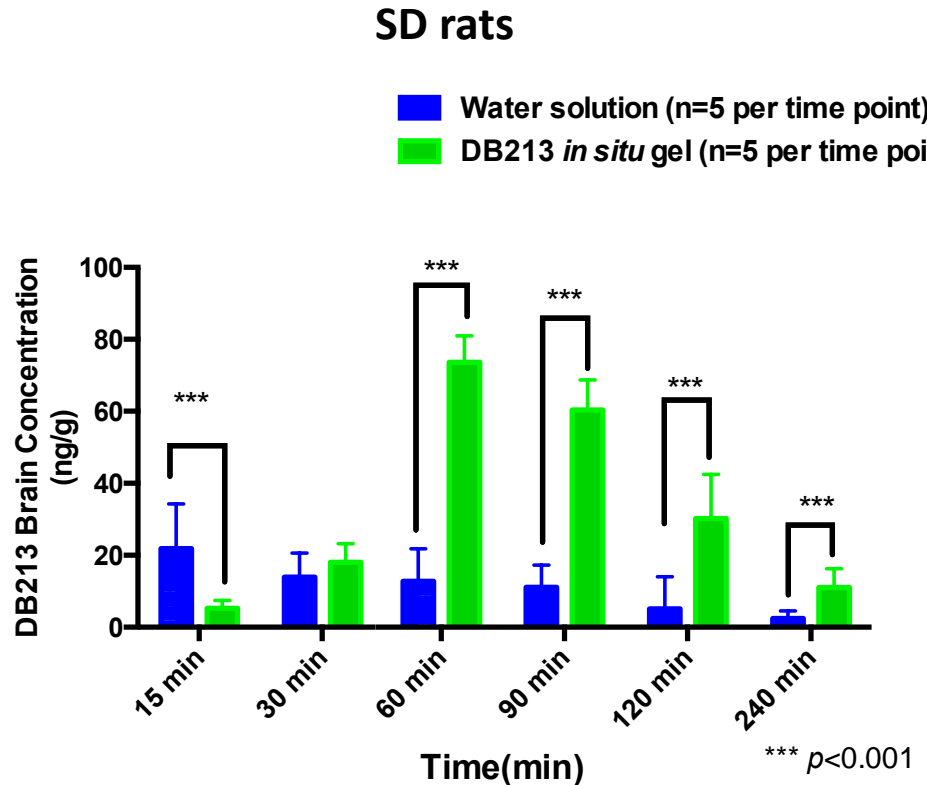
- $T_{sol-gel}$: 31°C
- *In vitro* release at 1 h: 75%
- MCT: 54 min

Performance Observations

- $T_{sol-gel}$: $31.6 \pm 0.4^\circ\text{C}$
- *In vitro* release at 1 h: $75 \pm 5.3\%$
- MCT: 60 ± 5 min

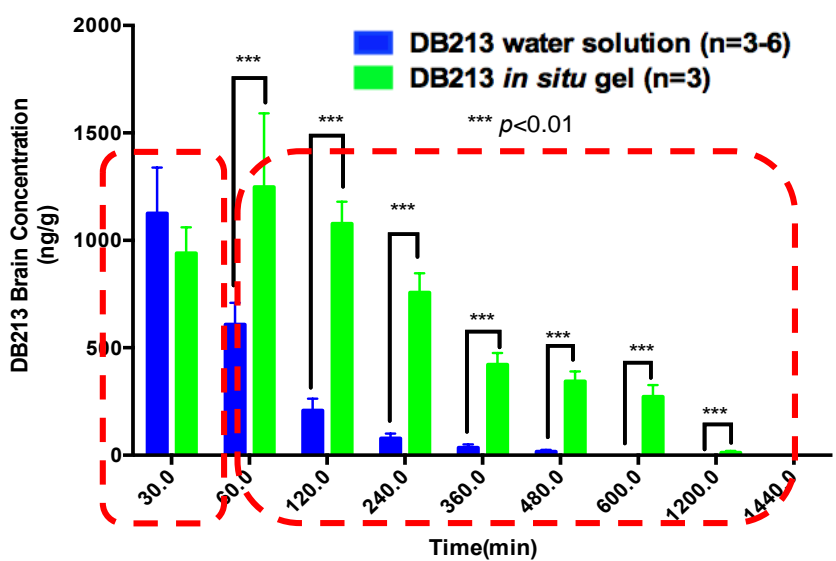
Based on DOE approach, DB213 in-situ gel with desired performance was developed.

Brain PK of DB213 delivered by in-situ gel in rats

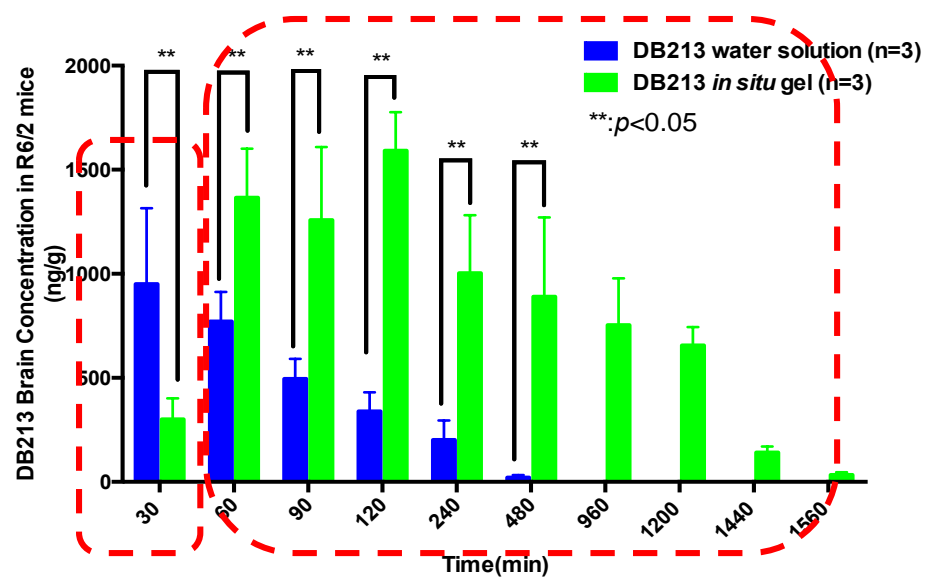


Brain PK of DB213 delivered by in-situ gel in mice

C57 mice



R6/2 mice

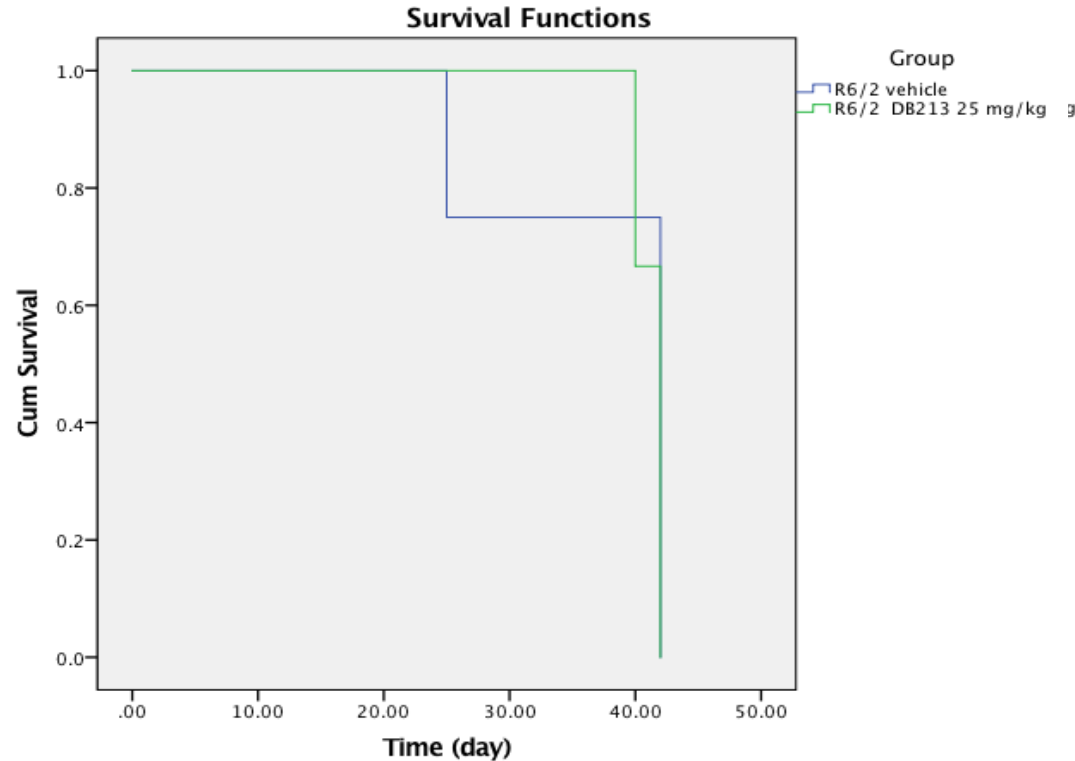


DB213 delivered by *in situ* thermosensitive gel demonstrated significant increase in its brain uptake in SD rats, C57 and R6/2 mice [17].

[17] Wang Q, Wong C H, Chan H Y E, et al. International journal of pharmaceutics, 2018, 539(1-2): 50-57.

IN-VIVO EFFICACY EVALUATION

Maximum tolerance dose(MTD) of DB213 delivered by in-situ gel in mice

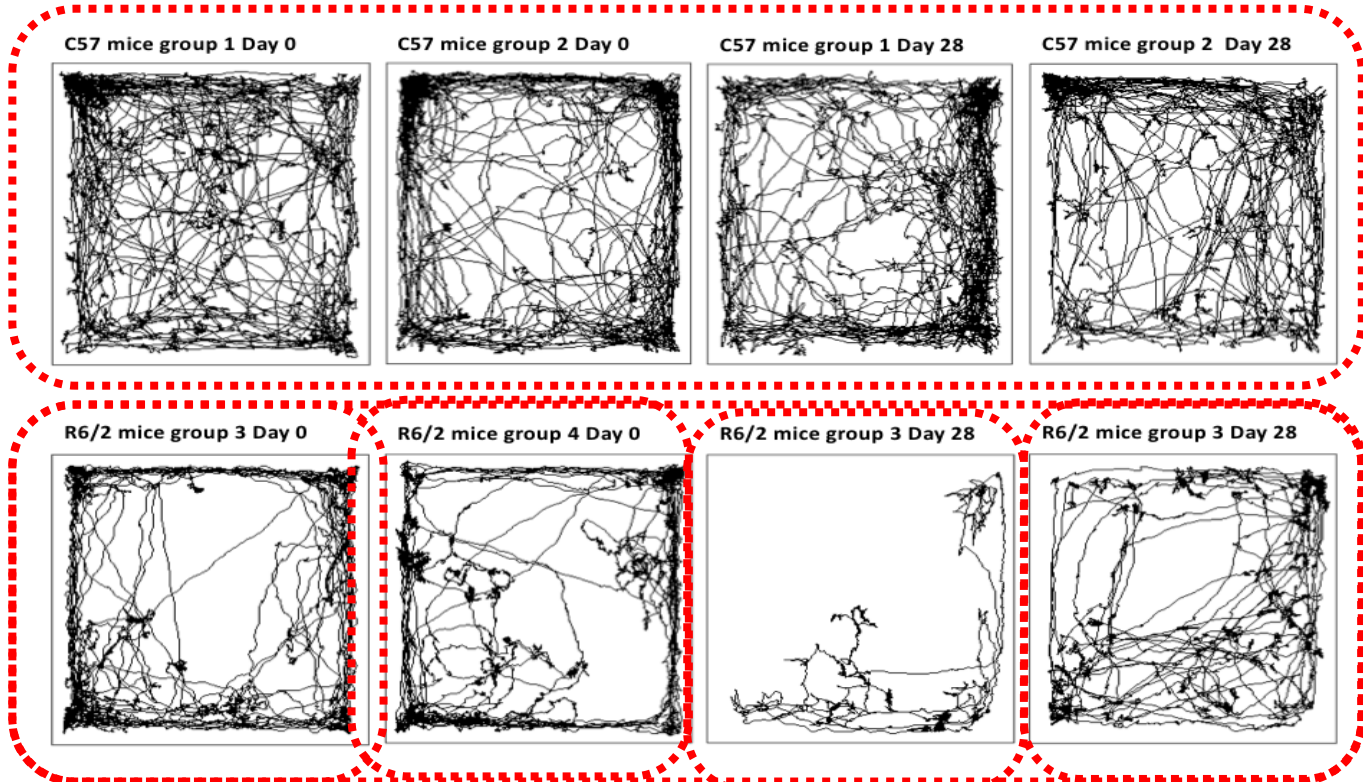


MTD of daily treatment of DB213 in-situ gel via IN up to 28 days was identified at 50 mg/kg for C57 mice and 25 mg/kg for R6/2 mice

Efficacy evaluation of DB213 in-situ gel in mice



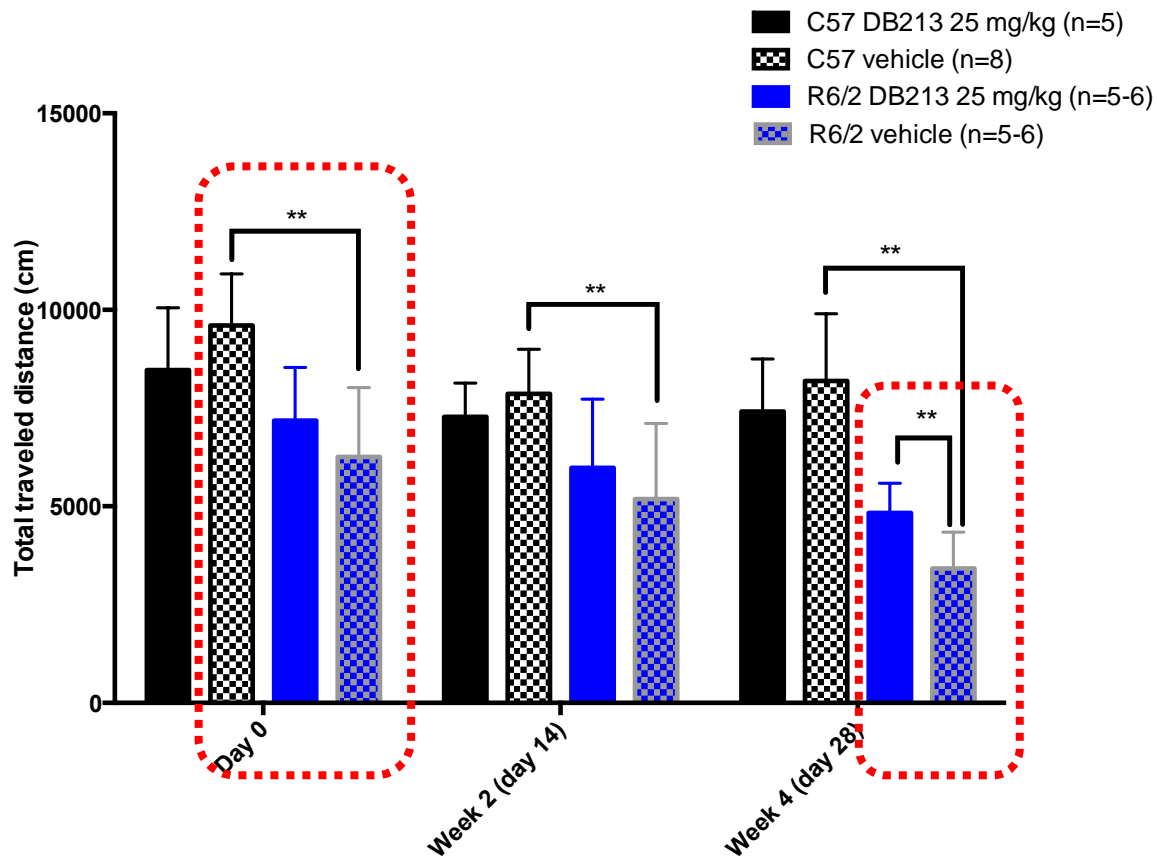
Open
field



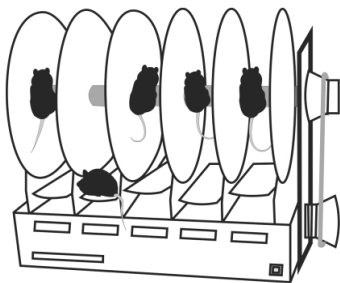
Efficacy evaluation of DB213 in-situ gel in mice



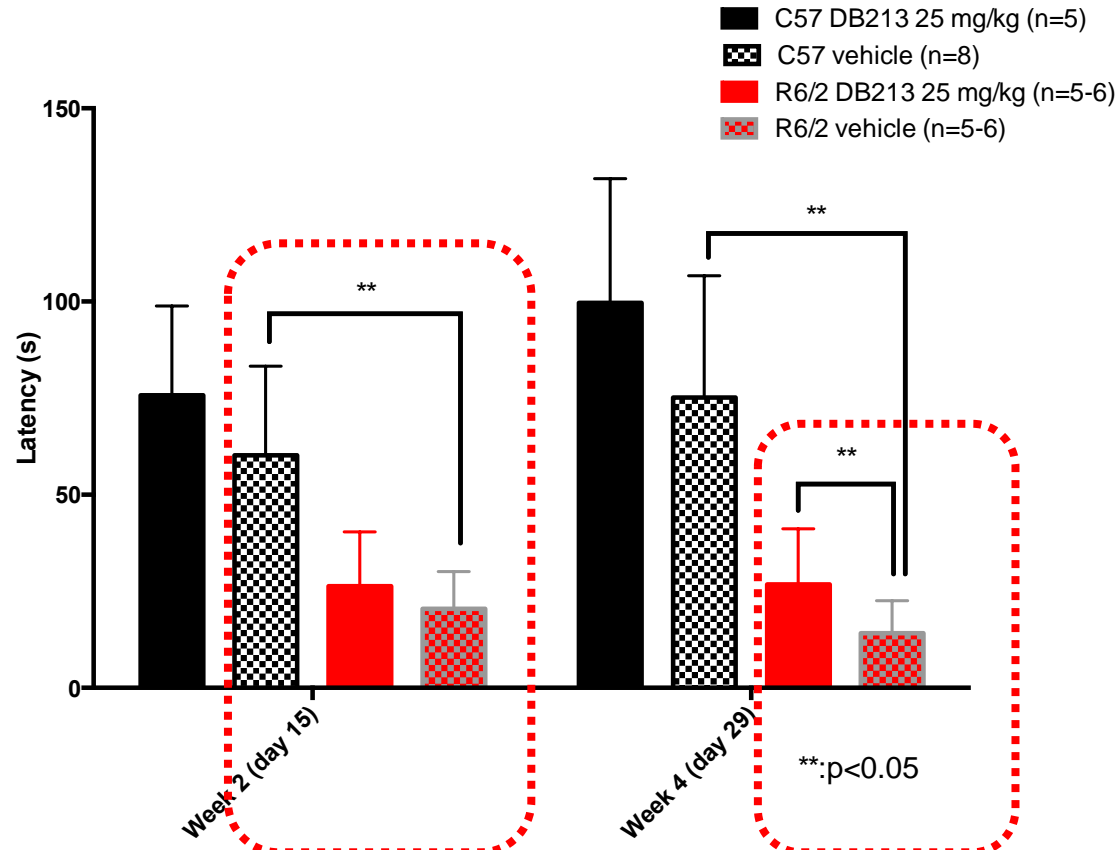
Open
field



Results: Efficacy evaluation of DB213 in-situ gel in mice



Rota-rod test



After 29-day treatment at 25 mg/kg (once daily) in R6/2 mice, DB213 in-situ thermosensitive gel group showed significant improvement in cognitive function (Open field test) and motor function (Rota-rod test) in comparison to vehicle group.



Brain-Targeting Delivery of Two Peptidylic Inhibitors for Their Combination Therapy in Transgenic Polyglutamine Disease Mice via Intranasal Administration

Mengbi Yang,[†] Qian Zhang,[‡] Qianwen Wang,[†] Kasper K. Sørensen,[§] Josephine T. Boesen,[§] Sum Yi Ma,[‡] Knud J. Jensen,[§] Kin Ming Kwan,^{‡,||} Jacky Chi Ki Ngo,[‡] Ho Yin Edwin Chan,^{‡,⊥} and Zhong Zuo^{*,†,◎}

[†]School of Pharmacy, The Chinese University of Hong Kong, Shatin, Hong Kong, SAR, China

[‡]School of Life Sciences, The Chinese University of Hong Kong, Shatin, Hong Kong, SAR, China

[§]Department of Chemistry, University of Copenhagen, Thorvaldsensvej 40, 1871 Frederiksberg, Denmark

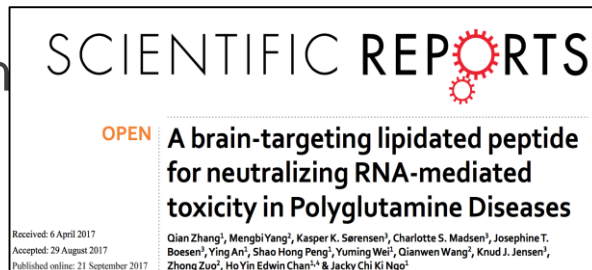
^{||}Partner State Key Laboratory of Agrobiotechnology, The Chinese University of Hong Kong, Shatin, Hong Kong, SAR, China

[⊥]Gerald Choa Neuroscience Centre, The Chinese University of Hong Kong, Shatin, Hong Kong, SAR, China

HOW ABOUT BIGGER MOLECULES?

Major Challenges

- Stability (in-vitro and in-vivo)
- Permeability;



香港中文大學
The Chinese University of Hong Kong

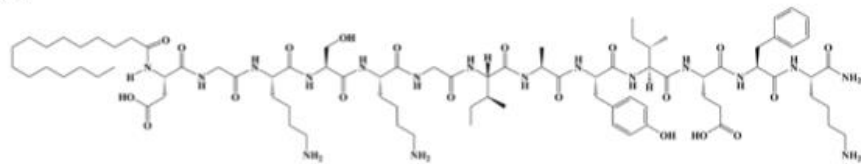


香港中文大學醫學院
Faculty of Medicine
The Chinese University of Hong Kong

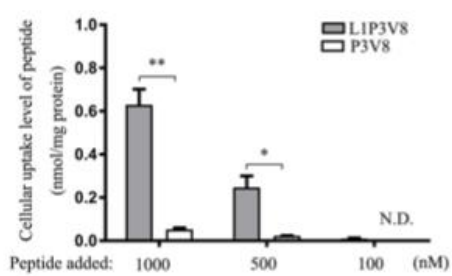


Lipidation of peptide

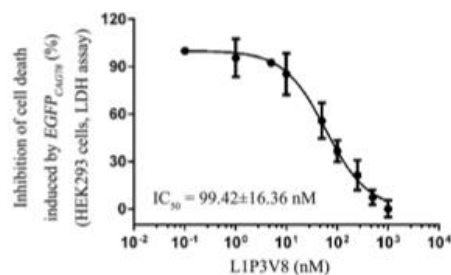
(a)



(b)



(c)



	Incubation Conc. (ng/mL)	Percentage of remained (%)	
		Incubation for 1 hr	Incubation for 3 hr
Plasma	2000	20.7 ± 3.3	98.8 ± 5.0***
	1000	8.6 ± 0.5	98.7 ± 3.9***
	500	<2.5 ^t	88.1 ± 4.9
Brain homogenate	2000	3.3 ± 0.6	45.0 ± 3.5***
	1000	4.0 ± 1.6	22.8 ± 1.2***
	500	<2.5 ^t	<20 ^t
		N/A	N/A
		73.8 ± 5.7	15.8 ± 0.7
		<20 ^t	<20 ^t

Table 2. Stability of P3V8 and L1P3V8 in different biological matrices after incubation at 37°C. Data are presented as mean ± S.E.M. for 5 independent experiments. ***Indicates $P < 0.001$, significant difference compared with P3V8. ^tIndicates the concentration was below the lowest limit of quantification (12.5 ng/mL for P3V8 and 100 ng/mL for L1P3V8). N/A indicates not applicable.

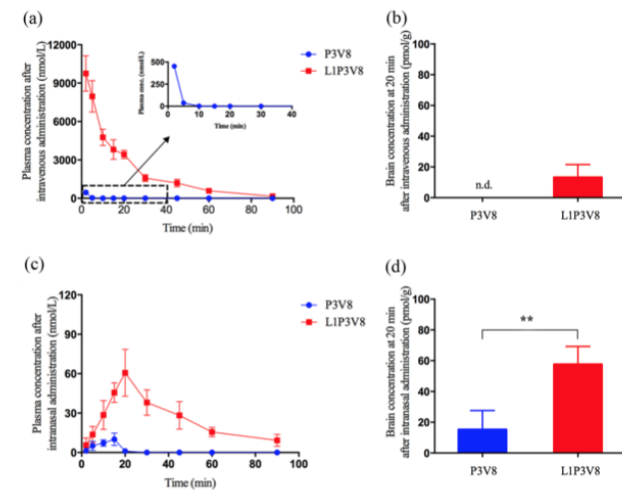


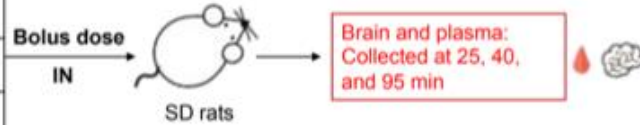
Figure 5. *In vivo* pharmacokinetic study and brain uptake of 3 μmol/kg P3V8 or L1P3V8 in rats. (a) Inhibitor plasma concentration-time profiles of P3V8 and L1P3V8 following intravenous administration. (b) Brain concentrations of P3V8 (n.d.: not detected) and L1P3V8 at 20 min after intravenous administration (c) Inhibitor plasma concentration-time profiles of inhibitors administered via the intranasal route after pre-treatment with 0.5% chitosan. (d) Brain concentrations of P3V8 and L1P3V8 at 20 min after intranasal administration. Data are presented as mean ± S.E.M. for 6 independent experiments. **Indicates $P < 0.01$.



Treatment Strategy

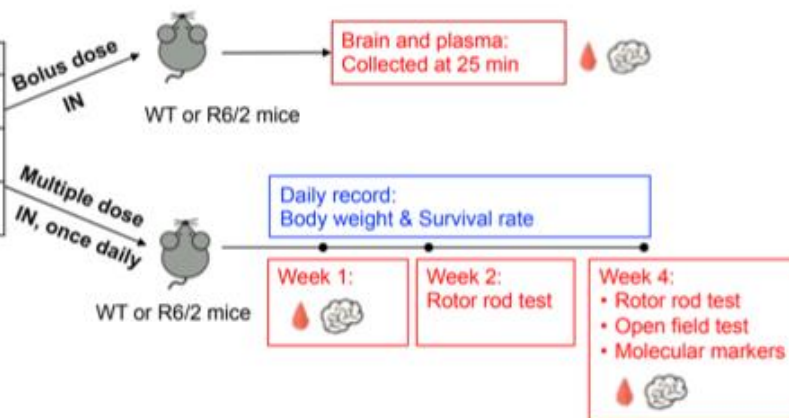
A Dosing scheme for rats (200 g):

min	Left nostril	Right nostril
0	Nil	Chitosan (0.5%, 20 μ L)
5	Nil	L1P3V8, 3 μ mol/kg (20 μ L)
10	QBP1, 8 μ mol/kg (in situ gel, 20 μ L)	Nil



B Dosing scheme for mice (25 g):

min	Left nostril	Right nostril
0	Nil	Chitosan (0.5%, 5 μ L)
5	Nil	L1P3V8, 6 μ mol/kg (10 μ L)
10	QBP1, 16 μ mol/kg (in situ gel, 5 μ L)	Nil



Choice of route of administration and formulation for QBP1

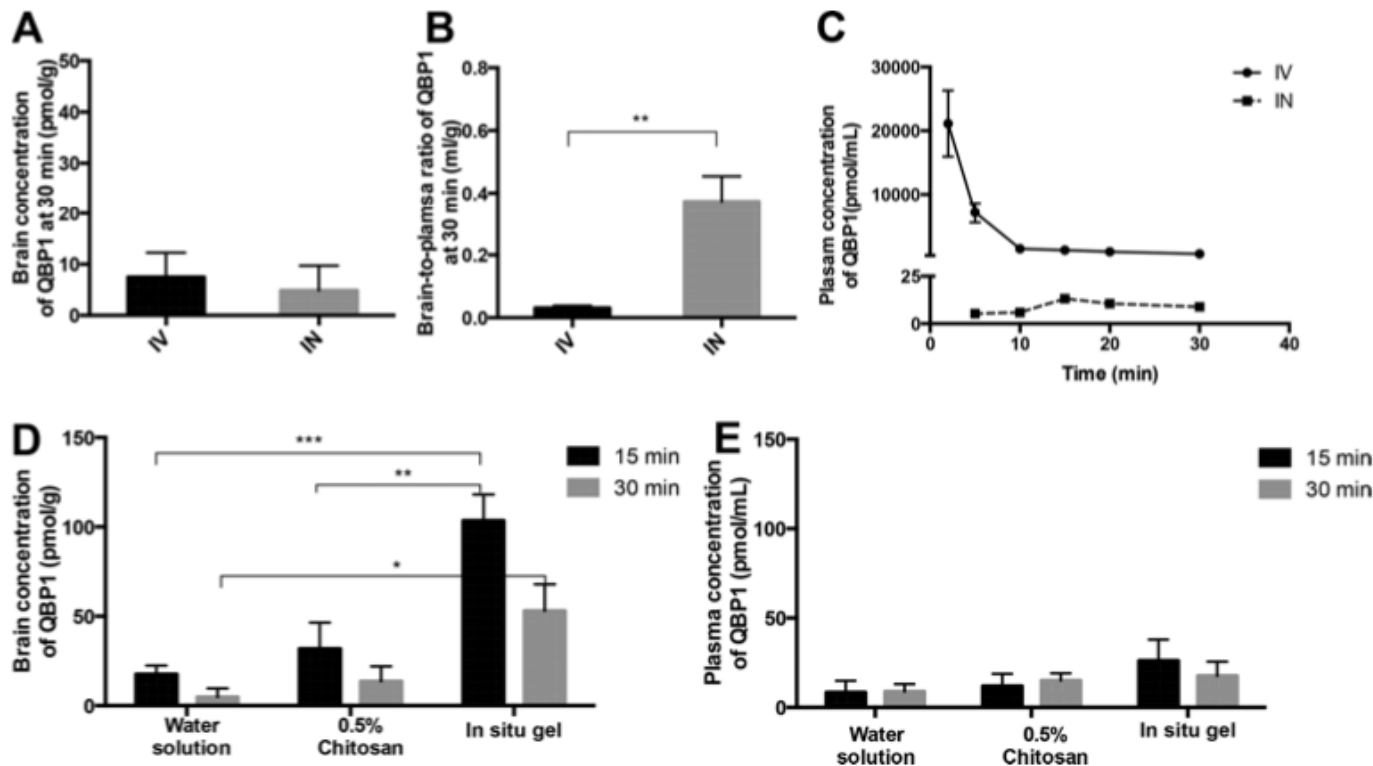


Figure 2. Comparison of brain uptake (A), brain-to-plasma ratio (B), and plasma concentration (C) of QBP1 after IV and IN administrations of its water solution at 8 $\mu\text{mol}/\text{kg}$ ($n = 5$) and further comparison of brain (D) and plasma (E) concentrations at 15 and 30 min after IN administrations of QBP1 (8 $\mu\text{mol}/\text{kg}$) in water solution ($n = 5$), 0.5% chitosan ($n = 6$), and in situ gel with 0.5% chitosan ($n = 6$) on SD rats. ***, $p < 0.001$; **, $p < 0.01$; *, $p < 0.05$ significant difference.

Evaluation of the efficacy for combination treatment

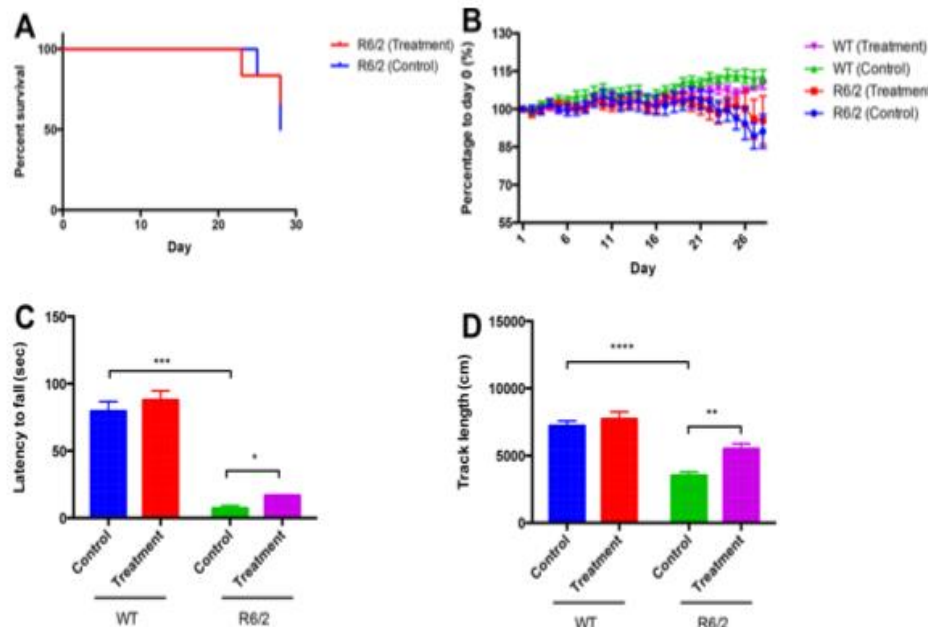


Figure 5. Therapeutic efficacy evaluation of a 4-week daily IN cotreatment of L1P3V8 (6 $\mu\text{mol/kg}$, pretreated with 0.5% chitosan) and QBP1 (16 $\mu\text{mol/kg}$, in situ gel) in WT and R6/2 mice ($n = 5-6$) via monitoring of survival rate of R6/2 mice (A), body weight changes during 4-week treatment on WT and R6/2 mice (B), latency to fall in rotor rod test at the end of week 4 on WT and R6/2 mice (C), and track length of 30 min open field test at the end of week 4 (D). ****, $p < 0.0001$; ***, $p < 0.001$; **, $p < 0.01$; *, $p < 0.05$ significant difference.

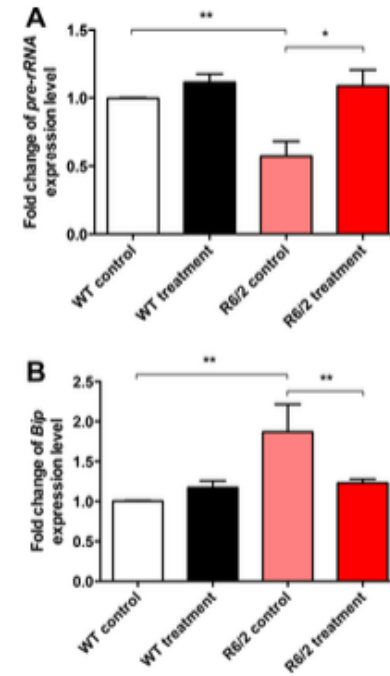


Figure 6. Cotreatment of L1P3V8 and QBP1 in R6/2 mice suppressed in both expanded CAG RNA and PolyQ protein-induced toxicity ($n = 4-6$) as demonstrated by the restoration of the pre-rRNA expression level (A) and suppression of the *Bip* induction level (B) in brain. Data for real-time PCR were normalized to WT control. **, $p < 0.01$; *, $p < 0.05$ significant difference.



Take home message



香港中文大學
The Chinese University of Hong Kong



香港中文大學醫學院
Faculty of Medicine
The Chinese University of Hong Kong



Acknowledgments

The Chinese University of Hong Kong

School of Pharmacy

- Dr. Yanfeng Wang
- Dr. Eric Wong
- Dr. Chores QW Wang
- Miss Shu Wang
- Dr. SK Wo
- Dr. Mengbi Yang
- Dr. Shuai Qian
- Dr. Yufeng Zhang

Department of Medicine and Therapeutics

- Prof. Brian Tomlinson

Department of Chemistry

- Dr. Ho, CY
- Miss He, LS

Department of Psychiatry

- Prof. Wing, YK

School of Life Science

- Prof. Edwin Chan & his team

Hong Kong Polytechnic University

- Prof. Han, YF & his team

Comprehensive Drug Enterprises Ltd, Hong Kong

- Dr. Benjamin Lee

Western Univ. of Health Sciences, USA

- Prof. Moses S.S. Chow

Research Funds from:

- University Grant Council of Hong Kong SAR;
- Innovation Technology Fund, HK SAR



joanzuo@cuhk.edu.hk